MODEL FOR DETECTION AND ASSESSMENT OF ABIOTIC STRESS CAUSED BY URANIUM MINING IN EUROPEAN BLACK PINE LANDSCAPES

Lachezar Filchev, and Eugenia Roumenina

Space Research and Technology Institute, Bulgarian Academy of Sciences (SRTI-BAS), Department of Remote Sensing and GIS, Sofia, Bulgaria;
e-mail: {roumenina / lachezarhf }(at)space.bas.bg

ABSTRACT

The article presents the results obtained from a study for detection and assessment of abiotic stress through pollution with heavy metals, metalloids, and natural radionuclides in European Black Pine (*Pinus nigra* L.) forests caused by uranium mining using ground-based biogeochemical, biophysical, and field spectrometry data. The forests are located on a territory subject to underground and open uranium mining. An operational model of the study is proposed. The areas subject to technogeochemical load are outlined based on the aggregate pollution index Z_c. Laboratory and field spectrometry data were used to detect the signals of abiotic stress at pixel level. The methods used for determination of stressed and unstressed black pine forests are: four vegetation indices (*TCARI*, *MCARI*, *MTVI* 2, and *PRI* 1) for stress detection, and the position, depth, asymmetry, and shift of the red-edge. Based on the „blue shift" and the depth and position of the red-edge, registered by the laboratory analysis and field spectral reflectance, it is established that coniferous forests subject to abiotic stress show an increase in total chlorophyll content and carotene. It has been found that the vegetation indices *MTVI* 2 and *PRI* 1, as well as the combination of vegetation indices and pigments may be used as a direct indicator of abiotic stress in coniferous forests caused by uranium mining.

INTRODUCTION

The significance and importance of vegetation stress is included in present-day plans, programmes, directives, and agendas of FAO, EC and other national and international authorities and governing bodies. Under the conditions of increased environmental pollution levels, plants accumulate high concentrations of harmful substances in their vegetative organs (1). Stress is largely perceived as a total response to environmental demands or pressures. This reaction can be either positive or negative (2). Furthermore, a simple dichotomy of stress to abiotic and biotic factors was given by (3). According to the authors the factors resulting in the occurrence of abiotic stress in coniferous plants are: wind, snowfalls, fires, drought, air pollution with aerosols and dust particles, heavy metals, pollution of soil and water with heavy metals, radionuclides and organic compounds (3). The physiological changes are expressed in the growth of organisms and functional disturbances, change in chlorophyll content and moisture provision in leaves, and chlorosis (2).

A classification of the abiotic stressors and their impact on the spectral characteristics of crop vegetation at particular wavelengths of the spectrum has been done recently (4). Using some indirect signs and correlation dependencies between structural and vegetation index (*VI*) images obtained by satellite imaging spectroradiometers, damages and stress may be identified and their scope and magnitude may be assessed. A set of narrow-band (about 2 nm) vegetation indices are being developed to register typical absorption elements characteristic of the availability of a given chemical element or compound in the studied object (5).

Abiotic stresses in mining environments are mainly caused by abiotic stressors such as salinity, pollution, and mineral deficiency/toxicity manifested in plant responses such as changed and altered biochemistry, chlorophyll content, altered growth and are detected by changing plant biochemical characteristics such as the Leaf Area Index (*LAI*) (3). Right after launching the Earth Resource and Technology Satellite (ERTS) or Landsat 1 in 1972, field and satellite data have been used extensively to study geological applications such as mineral exploitation and geological mapping. Satellite and airborne data was also used for studying chemical abiotic stress in conifers as a

DOI: 10.12760/01-2013-2-05

supplementary means for geological prospecting. For instance, in 1971 Howard et al. found that the increased reflectance at 810 nm for *Pinus ponderosa* is due to Cu and its compounds (3,6). Later on it was found that on Cu-Mo mineralization *Pinus contorta* communities exhibit higher reflectance at 670 nm and a smaller peak at 790 nm (7). A more general dependence between substrate mineralization and the higher reflectance of conifers from the grasses in the visible part of the spectrum was established (8). It was found that the second derivative of the spectral reflectance curve at 733 nm changes its shape due to chemical stress (9).

Numerous studies have shown the potential of airborne and satellite imaging spectrometry for detecting changes in foliar chemistry and stress detection. For example, airborne hyperspectral data obtained with the HyMap spectroradiometer showed that the chlorophyll concentration in needles of Norway spruce and young Balsam fir is positively correlated (r=0.99) with the vegetation index ANMB650–725 which can be used for stress detection (10). One of the most topical studies on the potentials of the future Hyperspectral Environment and Resource Observer (HERO) satellite mission for studying chemical vegetation stress in Canadian forests reveals the weaknesses of such a mission and outlines the potentials for improvement of its parameters in view of future studies (11). The actuality of the study is also in line with present developments and EU-wide projects which aim to observe the mining activities in the EU such as MINEO, HyperGreen, GMES4Mining, EUFODOS, and EO-Miners (12,13,14,15,16).

The major objective of the present study is to detect and to assess abiotic stress in European Black Pine (*Pinus nigra* L.) forests caused by uranium mining using ground-based biogeochemical, biophysical, spectrometric data. The subjects of the study are mono-culture landscapes of European Black pine (*Pinus nigra* L.) occupying the place of the natural oak vegetation (*Quercus* sp.), located on a territory subject to underground and open uranium mining on the Iskra mining section in the river basin of the Teyna River, a left tributary of the Iskur River, the Balkan Peninsula.

Study area

The river basin of the Teyna River is located between 42°50'N and 40°51'N latitude and 23°19'E and 23°20'E longitude and occupies an area of 4,775 km^2 with altitudes varying from 500 m a.s.l. at the discharge point of the Teyna River into the Iskur River to 964 m a.s.l. in the highest part of the water-catchment basin (17), (Figure 1).

The region falls entirely within the temperate-continental climatic belt, with a mesothermal climate (C) group after the climate classification of Köppen (18). The surface outflow of the Teyna River is small, reaching up to 1 m^3 per minute only during heavy rain and snow-melting. According to the global soil classification of the Food and Agricultural Organization (FAO) of the United Nations (UN) (19), the region is characterised by: Chromic Luvisols occupying 45.8% and Cambisols occupying 36.37% of the territory. The remaining 17.4% of the river basin are covered by bare soils or Anthrosols. According to the classification of the World Wildlife Fund (WWF) and the Digital Map of European Ecological Regions of the European Environment Agency (EEA), the river basin of the Teyna River completely falls within the ecoregion of the Balkan mixed forests, the Pale-Arctic ecozone (20). The dominating vegetation type is presented by mono-culture plants of Scots pine (*Pinus sylvestris* L.) and European Black pine (*Pinus nigra* L.) in the place of the natural oak (*Quercus* sp.).

Brief history of the mining section

The Iskra uranium mining section, located in the water-catchment basin of the Teyna River, features a total area of 4.87 ha (21,22). Falling within the section's boundaries are: 12 embankments, 1 quarry, and 2 technological sludge pans. The development of the deposit started in 1956 after the open-pit mining technique, while preparation of the deposits for underground mining was also carried out. The classical mining in the section ended in 1962. In 1984 the geotechnological mining was started, and was subsequently decommissioned in 1990. The technological liquidation, biological restoration, and reclamation started after 1994 based on Decree No.163/20.08.1992 of the Council of Ministers and Order No.56 of the Council of Ministers of 29.03.1994 (15,16). The environmental conditions in the studied region were additionally complicated by the correction of the river bed which caused almost total draining of the surface waters through adits in the Kisseloto

Ezero (Acid Lake) which is the place of uranium mining product sedimentation. The high soil-geochemical background with respect to some heavy metals exerts a direct influence on the concentrations and their redistribution across the natural complexes. Increased content of Pb, Cu, and Fe in soils of the region has been established, which was attributed to residual Pb pollution from the former Lead Mining and Processing Works in the Town of Novi Iskur, decommissioned in 1973 on account of the deteriorated ecological conditions (23).

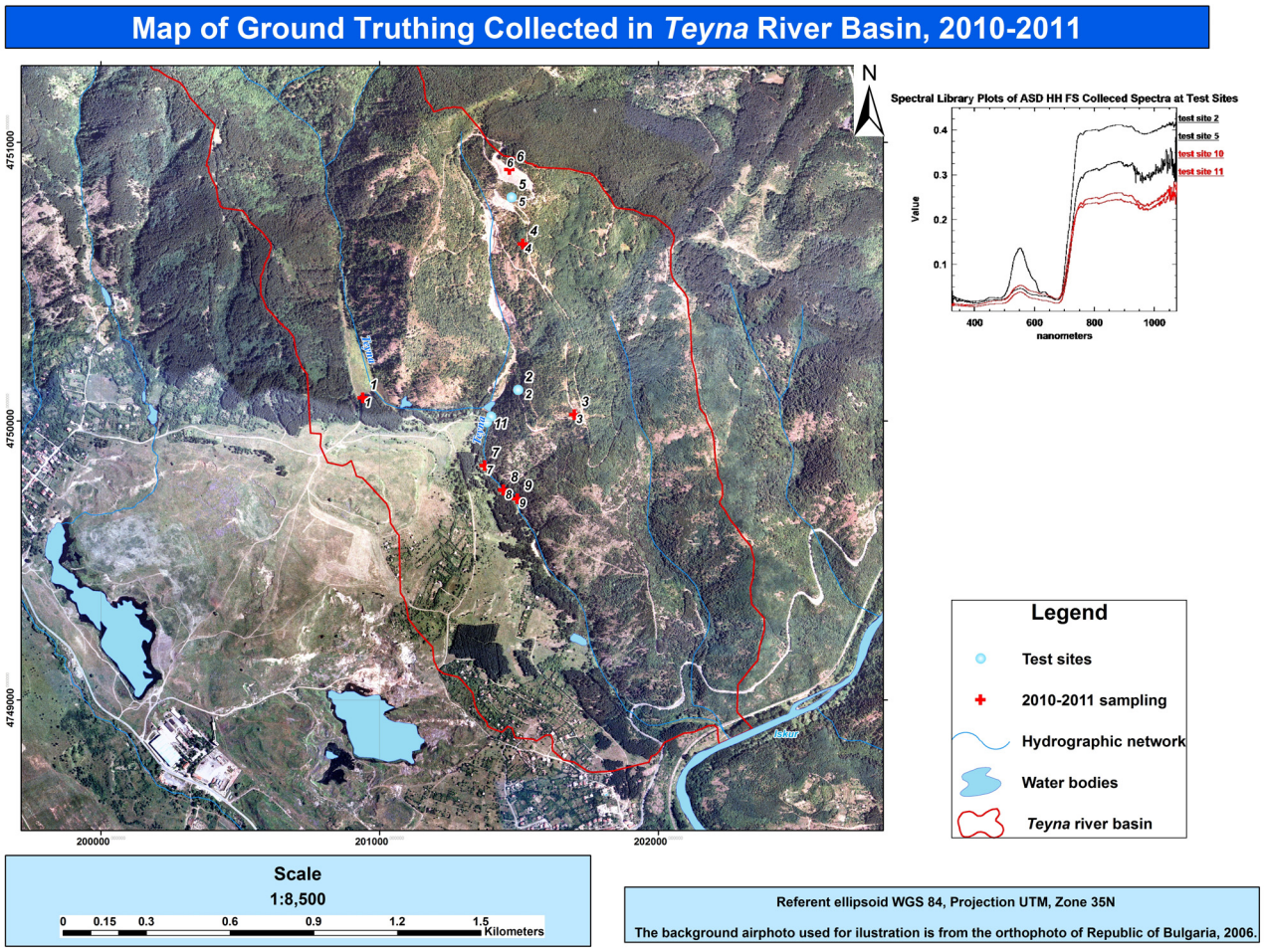

Figure 1: The study area with test sites and sampling points indicated.

METHODS

Two groups of data were used to identify the abiotic stress in coniferous vegetation in the examined region. The first includes data obtained from independent information sources, i.e., ground-based biogeochemical and biophysical data; the second group consists of ground-based field spectrometric data. A file geodatabase was composed in ArcGIS/ArcCatalog 9.2 for storing, visualizing, and managing the geospatial information.

Field Data

During the ground-based studies conducted in 2010-11 on the Iskra mining section, the following data were collected:

- GPS measurements were performed for an accurate georeferencing of field spectrometry measurements;
- Spectrometry measurements were conducted using the Hand Held FieldSpec (HH FS) Demo 1445 spectrometer of Analytical Spectral Devices (ASD).

The spectrometer operates within the range of 325-1075 nm of the Visible and Near-IR part of the spectrum (VNIR), using a 512-channel silicon photodiode detector covered by a separation filter (24).

In May 2011, a series of 130 field and laboratory spectrometric measurements were carried out. Four-fold measurements of the coniferous plant samples (two-year shoots) collected from four test sites were made. These measurements were:

- "hot-spot" field spectrometry measurements, taken from the light source direction - the Sunlight - and contact probe photodiode, using a 10° fore-optics. All spectra were taken during noon-time, i.e. the time-frame between 10h am and 14h pm, in cloud-free and sunny conditions
- laboratory spectrometry measurements of collected field specimens of Black pine needles from all test sites using the ASD contact probe
- Chlorophyll content using the method of Lichtenthaler (25). Spectra were bundled into a spectral library in ENVI file format (.sli) for the purpose of additional processing and classification
- *LAI* measurements have been taken in overcast sky conditions using an AccuPAR LP80 PARceptometer manufactured by DECAGON®. This was done as the overcast conditions had proven to give better results in determination of *LAI* for conifers with the AccuPAR LP80 PARceptometer
- Finally, the contents of heavy metals and metalloids (Cu, Zn, Pb, Ni, Co, Mn, and Cr) and natural radionuclides (^{235}U, ^{234}Th, ^{226}Ra, and ^{40}K) in soils and vegetation samples, as well as chlorophyll-*a*, chlorophyll-*b*, chlorophyll-*a+b*, and carotene were measured in laboratories licensed according to the international standards.

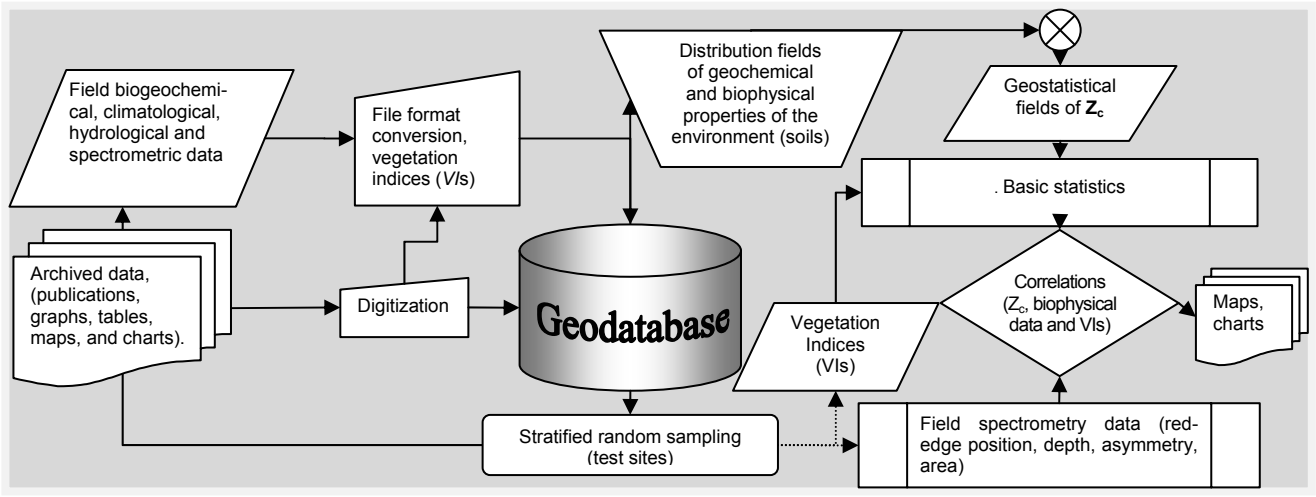

Figure 2: Flowchart of the model for detection and assessment of abiotic stress in coniferous landscapes.

According to the developed model (Figure 2), it was envisaged to perform the GIS analysis by integrating the results from the processing of the field spectrometry data at test site level. The test sites were chosen within landscape units characterised by exactly the same composition of natural and semi-natural environmental features. Some biometric parameters, such as tree density, age, and height were chosen to be homogeneous within the landscape units in order to eliminate the bias in collecting the spectra. The analysis is performed on four (two stressed and two non-stressed) out of 15 test sites as the two pairs of test sites appeared to be more contrasting in terms of aggregate pollution index Z_c values.

Aggregate pollution index Z_c

Forest maps from the regional forestry services of the town of Novi Iskar were used in order to establish the heavy metal, metalloids, and radionuclide pollution in the examined region. A stratified random sampling was made within European black pine forests to determine the test sites (*26*). This sampling resulted in 15 randomly distributed test sites within the coniferous forest stands. For

them, an assessment of the geo-chemical condition was made based on archive data and published materials, (27,28,29), as well as based on data from radiochemical, biogeochemical, and agrochemical analyses performed as a result of conducted field studies in the examined region during 2010–2011. The authors (18) established high values of the concentration coefficients (CCs) for the heavy metals Pb and Cu and of the Dispersion Coefficient (DC) for Ni, Zn, and Mn. From the calculated values of the biological absorption coefficient (A_x) it was established that Scots pine intakes Cu and Zn and European Black pine intakes Zn and Mn (19). In respect to the natural radionuclides, the strongest pollutant is Ra followed by U.

The assessment of the technogeochemical state of the examined coniferous landscapes for 1993 and 2011 was made using the aggregate pollution index Z_c with respect to the background concentrations (30,31,1):

$$Z_c = \sum_{i=1}^{n} K_c - (n-1) \tag{1}$$

where K_c is the technogenic concentration coefficient with K_c>1 (or 1.5), representing the ratio of heavy metal and metalloids concentrations and/or the specific activities of natural radionuclides in the surface soil horizon (0-20 cm) to the background concentrations and specific activities determined for the examined region:

$$K_c = \frac{C}{C_{background}} \tag{2}$$

n is the number of elements with K_c>1 (or 1.5). Territories with coefficient values of 50 to 60 and above have been found to be technogenically polluted. Based on the analysis of the values of Z_c, the authors conclude that in technogeochemical aspect, pollution was much higher (up to four times) in 1993-1996 compared to 2011, which is due to the freshly stopped uranium mining activity in the region.

The distribution fields of Z_c were made using the Geostatistical Analyst Extension in ArcInfo/ArcGIS 9.2. The interpolation method used for calculating the *CC*, *DC*, K_c, and Z_c was the Inverse Multiquadratic Function (*IMF*) from the set of the Radial Basis Functions (*RBF*), since the Root Mean Square Error (*RMSE*) has been shown to be the lowest as compared to other interpolation methods during cross-validation of the resulting layers.

Red-edge position

The VNIR part of the vegetation spectrum is characterised by five basic absorption lines (32). The electronic transitions of the photosynthetic pigments chlorophyll, xanthophylls, and carotene cause the absorption in the 400 to 700 nm range, while the bending and extension of the O-H link in the water molecule and other molecules cause absorption centred at 970 nm (33). A linear red-edge reflectance model (34) is used in this study:

$$R_{red-edge} = \frac{\rho_{670} - \rho_{780}}{2} \tag{3}$$

The position of the red-edge wavelength of the electromagnetic spectrum is given by (6):

$$\lambda_{red-edge} = 700 + 40\left(\frac{R_{red-edge} - \rho_{700}}{\rho_{740} - \rho_{700}}\right) \tag{4}$$

Vegetation Indices

Out of the available nearly 150 published Vegetation Indices (*VI*), only about 30 have been tested systematically (22,35). In the present study, four narrowband out of 30 narrowband *VI* were chosen and used to determine abiotic stress in coniferous landscapes (Table 1). The choice of the four indices was imposed due to their higher correlation coefficients with the field collected and laboratory analysed pigments data. After that the ENVI .sli spectral library containing the averaged spectra of the test sites was used as an input to the *VI* estimation using standard ENVI spectral math functions and additional IDL scripting. The ENVI .sli data format is useful for storing and managing field spectra as well as for data processing and visualisation.

Table 1: Vegetation indices used for determination of the abiotic vegetation stress.

Vegetation index	Equation	Source
Modified Chlorophyll Absorption in Reflectance Index (*MCARI*)	$MCARI = \left[\left(R_{700} - R_{670}\right) - 0.2\left(R_{700} - R_{550}\right)\right]\frac{R_{700}}{R_{670}}$	(36)
Transformed *CARI* (*TCARI*)	$TCARI = 3\left\{\left[\left(R_{700} - R_{670}\right) - 0.2\left(R_{700} - R_{550}\right)\right]\frac{R_{700}}{R_{670}}\right\}$	(37)
Modified Triangular Vegetation Index 2 (*MTVI* 2)	$MTVI2 = \frac{1.5\left[1.2\left(R_{800} - R_{550}\right) - 2.5\left(R_{670} - R_{550}\right)\right]}{\sqrt{\left(2R_{800} + 1\right)^2 - \left(6R_{800} - 5\sqrt{R_{670}}\right) - 0.5}}$	(38)
Photochemical Reflectance Index 1 (*PRI* 1)	$PRI1 = \frac{R_{528} - R_{567}}{R_{528} + R_{567}}$	(39)

Statistical analysis

Correlation (Pearson) and regression analysis between the laboratory measured pigments, *ASD HH FS VI*, and Z_c values were carried out. A set of dendrograms was prepared according to the hierarchical clustering (Ward) method using the field spectrometry data, the laboratory measured pigments, and ground-measured *LAI*.

RESULTS AND DISCUSSION

The areas subject to technogenic geochemical pollution were delineated based on the Z_c. Coniferous landscapes subject to abiotic stress were reclassified into four classes according to their Z_c values (Table 2).

Table 2: Classes of the agregate pollution coefficient Z_c in soils.

	1st class	2nd class	3rd class	4th class
Class names	Unstressed	Moderately stressed	Stressed	Heavily stressed
Z_c values	0÷10	10÷20	20÷50	>50

According to the classification in 2011 only stressed (test sites 10 and 11) and unstressed (test sites 2 and 5) coniferous landscapes were identified in the study area.

Position and depth of the red-edge determined by field and laboratory data

The positions of the red-edge in the visible part of spectrum (VIS) for field- and laboratory-measured spectral reflectance of samples of two-year black pine needles were determined with the multiplication method of the maximal value of the absorption line depth using the software add-on for ENVI developed by F. Van der Meer. In field spectra, the position of the red edge with stressed plants (the deepest part of the continuum removed spectrum) is shifted slightly towards the orange and green part of the spectrum, i.e., the so called “blue shift”. With healthy plants, it is at about 683-685 nm, while it is at about 674 nm with stressed ones (Table 3).

Table 3: Depth and position of the red edge in the VIS part of spectrum for ASD HH FS.

Test site No.	Red-edge position λ (nm)	Depth	Area	Asymmetry
2	683.00	0.17	19.19	1.07
5	685.00	0.33	59.92	2.36
10	674.00	0.71	193.02	5.60
11	676.00	0.87	270.30	5.88

The depth, area and asymmetry of the absorption line at about 685-700 nm is significantly better expressed with stressed plants than with non-stressed ones.

Relationships between Biophysical, Geochemical Data, and *VI*

Correlation and regression relationship with the values of the ground-measured *VI*, *LAI*, chlorophyll-*a*, chlorophyll-*b*, chlorophyll *a*+*b*, and carotene was derived. Very strong positive relationships with Z_c were established with the pigment content, and very poor negative relationship of *LAI* with Z_c (Table 5).

Table 5: Pearson correlation coefficients (r) for Z_c, chlorophyll-a, chlorophyll-b, chlorophyll a+b, carotene, and LAI (α = 0.05).

Variable	**Z_c**
Chlorophyll *a* (mg/kg)	0.95
Chlorophyll *b* (mg/kg)	0.95
Chlorophyll *a*+*b* (mg/kg)	0.95
Carotene (mg/kg)	0.96
LAI	-0.24
TCARI	-0.03
MCARI	-0.80
MTVI 2	0.85
PRI 1	0.74

From the *VI* under investigation *TCARI*/*MCARI* have negative relationships with Z_c, whereas Z_c has only strong positive relationship with *PRI*1 and *MTVI* 2. The strongest positive correlation is found for Z_c and carotene, followed by Z_c and chlorophyll, then *MTVI* 2 and *PRI* 1. A reverse correlation is found between *MTVI* 2 and Z_c and accordingly between *MCARI* and Z_c.

The distances at which the clusters are grouped are presented in Table 6. In the table *TCARI* and *MCARI* values group their first cluster relatively farther than Z_c, *MTVI* 2, and *PRI* 1. These results also support the conclusions for the *VI*'s performances for abiotic stress detection drawn from visual comparison between dendrogrammes presented in Figure 2.

Table 6: Cut-off distances for clustering of Z_c, chlorophyll-a, chlorophyll-b, chlorophyll a+b, carotene, LAI, and the chosen VI dendrograms.

Clusters	**1**	**2**	**3**
Chlorophyll-*a* (mg/kg)	1.65	0.46	0.17
Chlorophyll-*b* (mg/kg)	1.66	0.43	0.17
Chlorophyll *a*+*b* (mg/kg)	1.65	0.46	0.17
Carotene (mg/kg)	1.66	0.46	0.05
LAI	1.62	0.52	0.26
TCARI	1.84	1.51	0.53
MCARI	1.84	1.51	0.53
MTVI 2	1.55	0.72	0.23
PRI 1	1.56	0.73	0.06
PC 1 - *VI* and pigments	1.76	1.44	0.88
Z_c	1.72	0.11	0.00

In Figure 3 below the clustering distances are presented graphically on the dendrograms.

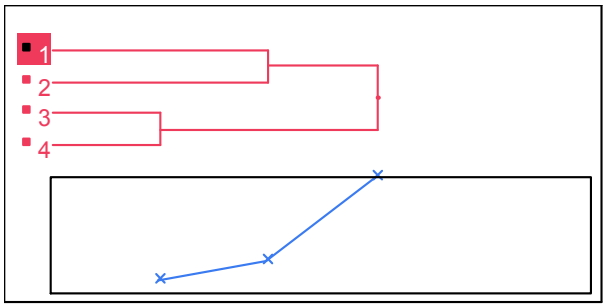

Chlorophyll *a+b*

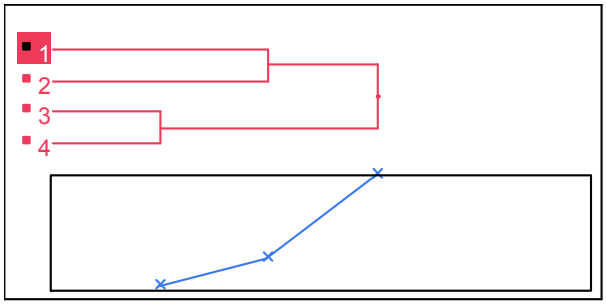

Carotene

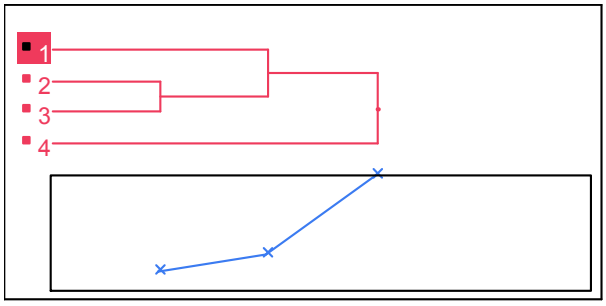

LAI

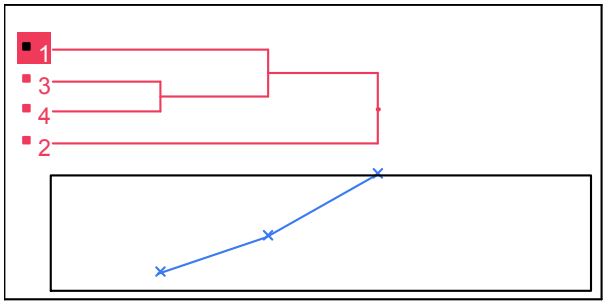

MTVI 2

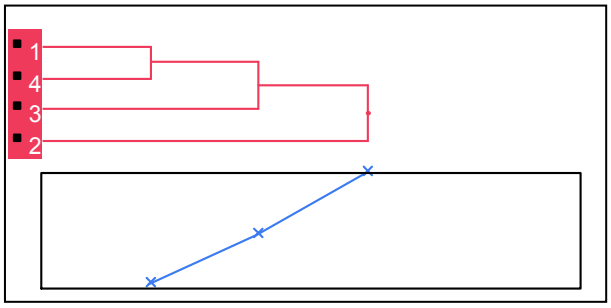

PRI 1

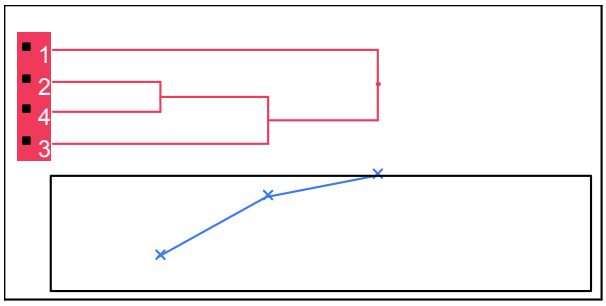

TCARI/MCARI

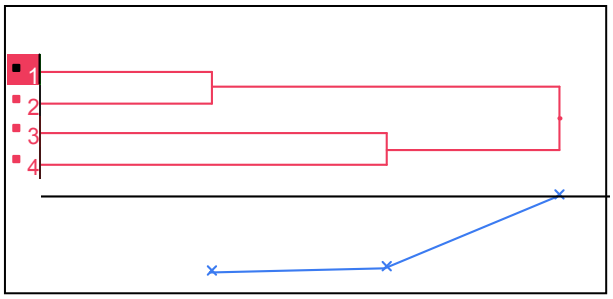

PC 1 - VI and pigments

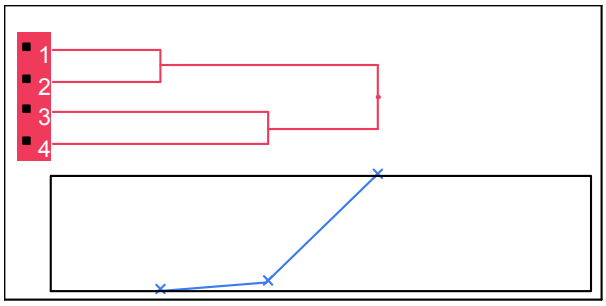

Z_c

Figure 3: Dendrograms of ASD HH FS VI, pigments, LAI, PC 1, and Z_c.

The numbers 1, 2, 3, and 4 on the dendrograms correspond to the four test sites 2, 5, 10, and 11 accordingly. The values of the pigments are grouped similar to the initially separated classes of stressed (test sites 10 and 11) and unstressed (test sites 2 and 5) coniferous landscapes, while the remaining *VI* values are not grouped in the same way. Only the *MTVI* 2 value grouping resembles the Z_c and pigments grouping, however, not being able to distinguish between the initially tested groups. The values of *VI* with pigments are grouped similar to the grouping of chlorophyll-*a*, chlorophyll-*b*, carotene, and Z_c. Therefore, the *VI* (*TCARI*/*MCARI*, *MTVI*2, and *PRI* 1) and pigments (chlorophyll-*a*, chlorophyll-*b*, and carotene) clusters in the same way as the aggregated pollution index Z_c.

Nevertheless, the similar clustering pattern is only possible in the presence of pigment content data. Therefore, although there is a strong correlation between the *MTVI* 2 and *PRI* 1 and Z_c, the tested *VI* have no distinctive potential between tested groups of stressed and non-stressed vegetation if no supplementary pigment data is present. This conclusion is also supported by the fact that *PC* 1 clustering, which accounts for 71.4% of the *VI* and pigments data, i.e., field spectra and laboratory data, is almost the same as of the pigment data.

CONCLUSIONS

Using the field and satellite spectrometry data, the *VI* and biogeochemical data, it was established that coniferous forests are subject to abiotic stress caused by uranium mining. It was found that, in field spectra, the position of the red edge with stressed plants is shifted slightly towards the orange and green part of the spectrum, i.e. the so called "blue shift". With healthy plants this shift is at 683-685 nm, while it is at about 674 nm with stressed ones. Furthermore, the stressed coniferous plants feature a non-specific stress reaction or „exstress". It features an increase of the total chlorophyll and carotene content with increasing total pollution coefficient Z_c.

However, this conclusion is true at a certain point when tree growth becomes impossible because of high level pollution followed by a lethal outcome. It has also been found out that the *VI* such as *MTVI* 2 (r=0.85) and *PRI* (r=0.74) may be used as a direct indicator of abiotic stress caused by uranium mining in coniferous landscapes. The correlation between the four obtained *VI* and Z_c led to the conclusion that most *VI*, using chlorophyll absorption lines, show a very strong inverse correlation relationship with the total chlorophyll content, chlorophyll-*a* and chlorophyll-*b* content while Z_c features show a very strong positive relationship with pigment contents.

Nevertheless, it was also found that the *VI* without additional pigment concentration data for the pine needles are not sufficient to clearly distinguish between classes of stressed and non-stressed vegetation. In conclusion, the study will continue with an investigation of the narrowband *VI* which feature the most distinctive relationship between *VI* and the modelled Z_c values. Also, future studies of this topic will definitely benefit from a more rigorous and versatile model for pollutant distribution in soils and reclaimed lands.

ACKNOWLEDGMENTS

The biogeochemical analysis of soils and coniferous vegetation are financed under the *Enhancing the Qualification and Retaining a Young Scholars' Team in the Field of Aerospace Technologies as a Prerequisite for Monitoring and Preservation of the Environment and Prevention of Damages Caused by Natural Disasters Project* under Contract No.BG051PO001/07/3.3-02/63/170608 within the Human Resource Development Operative Programme of the Ministry of Education, Youth and Science (MEYS) of the Republic of Bulgaria, awarded to Chief Assistant Dr. L. Filchev. The field spectrometric studies were carried out using ASD HH FS Demo 1445 awarded for temporary use under the Alexander Goetz Instrument Support Program (AGISP) 2011 financed by ASD Inc. and IEEE Geoscience and Remote Sensing Society (GRSS). The authors are deeply grateful to Ms Luba Kraleva, M.Sc. for final English language corrections of the manuscript.

REFERENCES

1 Prasad M N V, 2004. Heavy metal stress in plants - from biomolecules to ecosystems (Springer - Narosa Publishing House) 462 pp.

2 Gale Encyclopedia of Medicine, 2008. http://medical-dictionary.thefreedictionary.com/stress (Last date accessed: 15 Nov 2012)

3 Jones H G & P Schofield, 2008. Thermal and other remote sensing of plant stress. General and Applied Plant Physiology, 34: 19-32

4 Chi G Y, Y Shi, X Chen, J Ma & T H Zheng, 2011. Effects of metal stress on visible/near-infrared reflectance spectra of vegetation. Advanced Materials Research, 347: 2735-2738

5 Howard J, R Watson & T Hessin, 1971. Spectral reflectance properties of *Pinus ponderosa* in relation to copper content of the soil-Malachite mine, Jefferson County, Colorado (Ponderosa pine foliage visible and near IR spectra, investigating soil copper contents effect on foliage spectral reflectance). In: 7th International Symposium on Remote Sensing of Environment (University of Michigan, Ann Arbor, Mich., USA)) 285-297

6 Van der Meer F & S M de Jong, 2001. Imaging Spectrometry: Basic Principles and Prospective Applications (Springer) 403 pp.

7 Birnie R W & J D Dykstra, 1978. Application of remote sensing to reconnaissance geologic mapping and mineral exploration. 12th International Symposium on Remote Sensing of Environment, Vol. 2 (Environmental Research Institute of Michigan, Ann Arbor, Michigan, USA) 795-804

8 Horler D N H, J Barber & A R Barringer, 1980. Effects of heavy metals on the absorbance and reflectance spectra of plants. Remote Sensing of Environment, 1: 121-136

9 Merton R N, 1999. Multi-temporal Analysis of Community Scale Vegetation Stress with Imaging Spectroscopy. PhD Thesis (University of Auckland) 491 pp.

10 Kupková L, M Potůčková, K Zachová, Z Lhotáková, V Kopačková & J Albrechtová, 2012. Chlorophyll determination in silver birch and scots pine foliage from hyperspectral data. EARSeL eProceedings, 11: 64-73

11 Peddle D R, R B Boulton, N Pilger, M Bergeron & A Hollinger, 2008. Hyperspectral detection of chemical vegetation stress: Evaluation for the Canadian HERO satellite mission. Canadian Journal of Remote Sensing, 34: 1712-7971

12 Marsh S H, C Cotton, G Ager & D Tragheim, 2000. Detecting mine pollution using hyperspectral data in temperate, vegetated European environments. In: Proceedings of the 14th ERIM Thematic Conference (Las Vegas, NV, USA) 552-555

13 MINEO, 2003. Assessing and Monitoring the Environmental Impact of Mining Activities in Europe Using Advanced Earth Observation Techniques, Final Report - Section 6: Detailed report, IST–1999-10337. http://www2.brgm.fr/mineo/final.htm (last date accessed: 03 Oct 2013)

14 Benecke N, K Zimmermann, A Müterthies, K Pakzad, S Stephan, J Kateloe, A Preuße, E Pebesma & T Prinz, 2012. GMES4Mining - Innovative Geoservices for Exploration and Monitoring of Mining Areas. In: Proceedings of the 7th International Symposium AIMS 2012 (Aachen, Germany) (in press)

15 EUFODOS FP7 Project. http://www.eufodos.info/content/eufodos-fp7-project (last date accessed: 03 Oct 2013)

16 Earth Observation in the frame of EO-MINERS - Overview of remote sensing methods, sensors and applications. http://www.eo-miners.eu/earth_observation/eo_eof_msa_remote_sensing_apps.htm (last date accessed: 08 Oct 2013)

17 Filchev L, 2009. Design of digital landscape model of the Teyna river watershed for the purposes of landscape-ecological planning. In: 5th Scientific Conference with International Participation Space, Ecology, Nanotechnology, Safety (SENS 2009) (SRI-BAS, Bulgaria) 168-173

18 Kottek M, J Grieser, C Beck, B Rudolf & F Rubel, 2006. World map of the Koppen-Geiger climate classification updated. Meteorologische Zeitschrift, 15: 259-263

19 Panagos P, A Jones, C Bosco, & P S S Kumar, 2011. European digital archive on soil maps (EuDASM): preserving important soil data for public free access. International Journal of Digital Earth, 4: 434-443

20 Olson D M, E Dinerstein, E D Wikramanayake, N D Burgess, G V N Powell, E C Underwood, A J D'amico, H E Illanga Itoua, J C Strand, C J Morrison, T F L Allnutt, T H Ricketts, Y Kura, J F Lamoreux, W W Wettengel, P Hedao & K R Kassem, 2001. Terrestrial ecoregions of the world: a new map of life on earth. BioScience, 51: 933-938

21 Roumenina E, N Silleos, G Jelev, L Filchev & L Kraleva, 2007. Designing a spatial model of land use impact dynamics caused by uranium mining using remote sensing and ground-based methods. Proceedings of the 3rd Scientific Conference with International Participation „Space, Ecology, Nanotechnology, Safety" (SENS) 2007 (SRI-BAS, Varna, Bulgaria) 179-184

22 Naydenova V & E Roumenina, 2009. Monitoring the mining effect at drainage basin level using geoinformation technologies. Central European Journal of Geosciences, 1: 318-339

23 Filchev L & I Yordanova, 2011. Landscape-geochemical investigations of the consequences from uranium-ore extraction in Taina river basin. Ecological Engineering and Environment Protection, 4: 14-22 (in Bulgarian)

24 Analytical Spectral Devices Inc., 2003. FieldSpec UV/VNIR HandHeld Spectroradiometer User Guide (ASD Inc.) 72 pp.

25 Zhang Y, J M Chen, J R Miller & T L Noland, 2008. Retrieving chlorophyll content in conifer needles from hyperspectral measurements. Canadian Journal of Remote Sensing, 34(3): 296-310

26 McCoy R M, 2005, Field Methods in Remote Sensing (The Guilford Press, New York, USA) 171 pp.

27 Simeonova A, J Ignatov & M Mladenov, 1993. Radiological Assessment of "Iskra" section at underground construction (DIAL Ltd. - Buhovo 1830) 77 pp. (in Bulgarian)

28 Banov M & B Hristov, 1996. Investigation and recultivation of lands of the vicinity of the Town of Buhovo damaged by Uranium mining. Problems of Geography, 1: 78-86 (in Bulgarian)

29 Georgiev P & S Grudev, 2003. Characteristic of Polluted Soils in the Uranium Mine section. Annual of University of Mining and Geology St. Ivan Rilski, 46: 243-248 (in Bulgarian)

30 Saet Y E, B A Revich & E P Yanin, 1990. Geochemistry of the Environment (Mir, Moscow, Russia) 335 pp. (in Russian)

31 Vodyanitskii Y N, 2010. Equations for assessing the total contamination of soils with heavy metals and metalloids. Eurasian Soil Science, Degradation, Rehabilitation, and Conservation of Soils, 43: 1184-1188

32 Curran P J, 1989. Remote sensing of foliar chemistry. Remote Sensing of Environment, 30: 271-278

33 Curran P J, J L Dungan, B A Macler, S E Plummer & D L Peterson, 1992. Reflectance spectroscopy of fresh whole leaves for the estimation of chemical concentration. Remote Sensing of Environment, 39: 153-166

34 Guyot G, F Baret & D J Major, 1988. High spectral resolution: determination of spectral shifts between the red and near infrared. International Archives of the Photogrammetry, Remote Sensing and Spatial Information Sciences, 1988, 27: 750-760

35 Verrelst J, B Koetz, M Kneubühler & M Schaepman, 2006. Directional sensitivity analysis of vegetation indices from multiangular chris/proba data. Proceedings of XXXVI ISPRS Symposium, Part 7

36 Daughtry C S T, L L Biehl & K J Ranson, 1989. A new technique to measure the spectral properties of conifer needles. Remote Sensing of Environment, 27: 81-91

37 Haboudane D, J R Miller, P J Zarco-Tejada & L Dextraze, 2002. Integrated narrow-band vegetation indices for prediction of crop chlorophyll content for application to precision agriculture. Remote Sensing of Environment, 81: 416-426

38 Haboudane D, J R Miller, E Pattey, P J Zarco-Tejada & I B Strachan, 2004. Hyperspectral vegetation indices and novel algorithms for predicting green LAI of crop canopies: Modeling and validation in the context of precision agriculture. Remote Sensing of Environment, 90: 337-352

39 Gamon J A, J Penuelas & C B Field, 1992. A narrow-waveband spectral index that tracks diurnal changes in photosynthetic efficiency. Remote Sensing of Environment, 41: 35-44